Study of the (α,t) Reaction in F^{19}†

LUISA F. HANSEN, H. F. LUTZ, MARION L. STELTS, JOSE G. VIDAL, AND JEROME J. WESOLOWSKI
Lawrence Radiation Laboratory, University of California, Livermore, California
(Received 9 January 1967)

The $F^{19}(\alpha,t)Ne^{20}$ reaction has been studied at 28.5 MeV. Angular distributions and absolute cross sections have been measured from 15° to 170° for transitions leading to the ground (0^+), 1.63-MeV (2^+), 4.25-MeV (4^+), and 4.97-MeV (2^-) states. The 5.63-MeV (3^-) and 5.80-MeV (1^-) levels were observed, but not resolved; this was also the case for the 7.02-MeV (4^-), 7.19-MeV (3^-), and 7.22-MeV (0^+) levels. The 6.75-MeV (0^+) level was barely excited in the reaction. The angular distributions of the tritons to all the final states in Ne^{20}, with the possible exception of the 4.97-MeV level, show the characteristics of a stripping mechanism. The possibility of intermediate inelastic excitations in the stripping to the 4.25-MeV level is discussed. The angular distributions have been fitted with a zero-range distorted-wave Born approximation, and ratios of spectroscopic factors have been compared with the predictions of the Nilsson model and Harvey's $SU(3)$ shell-model calculations for Ne^{20}.

INTRODUCTION

IN the past it has been suggested[1,2] that the (α,t) reaction is analogous to the (d,n) reaction with the advantageous feature of having a charged outgoing particle. It is expected that the same levels populated in the (d,n) reaction will be excited in the final nucleus by the (α,t) reaction, but because of the larger momentum carried by the α particle, the reaction will populate preferentially those levels with higher angular momentum.

The (α,t) reaction in F^{19} has been measured by Jahr[3] at 18.5 MeV and Kakigi[4] at 28.5 MeV. In the first work only the ground and first excited states were observed. In Kakigi's work the ground and first two excited states were measured for a few forward angles. Jahr, after comparing the larger cross sections observed in the $F^{19}(\alpha,t)Ne^{20}$ reaction with those measured for the $F^{19}(He^3,d)Ne^{20}$ reaction at 13.0 MeV, concluded that the (α,t) reaction did not proceed only by a stripping mechanism, but rather by a cluster exchange process.

The cluster picture of F^{19} as an O^{16} core plus a triton has been invoked by Sheline and Wildermuth[5] to account for the positive-parity states in F^{19}. Reactions such as (p,t) and (p,α) in F^{19} have been tentatively interpreted[6,7] as a result of exchange processes, as well as pickup processes. However, the theoretical fits obtained by Holmgren and Fulmer[7] with a distorted-wave Born-approximation (DWBA) stripping calculation were not conclusive; they were able to fit the data without including knockout, but the quality of the fittings did not eliminate the possibility of a cluster structure in the target nucleus.

In the present work the $F^{19}(\alpha,t)Ne^{20}$ reaction has been studied using a zero-range DWBA stripping calculation,[8] and fair agreement with the experimental angular distributions for the ground state and two first excited states was found. No attempt was made to evaluate contributions to the reactions from other reaction modes.

The $F^{19}(\alpha,t)Ne^{20}$ reaction to the second excited state in Ne^{20} (4^+) shows evidence of contributions from processes other than direct stripping. Single-particle stripping alone could not account for the relatively large cross section observed for this level, since this would imply the presense of a rather large $1g$ component in the wave function of Ne^{20}. The calculations[9–13] on Ne^{20} do not include any $1g$ amplitude, and more complete calculations predict this contribution to be rather small.[14]

The ratios of spectroscopic factors of the 1.63- and 4.25-MeV levels to the ground state in Ne^{20} were obtained. They are compared with the calculated values, using Nilsson's collective model,[9] and with the spectroscopic factors calculated by Harvey,[15] using the $SU(3)$ classification of the shell model.

EXPERIMENTAL SET UP

The angular distributions of the $F^{19}(\alpha,t)Ne^{20}$ reaction have been measured at 28.5 MeV with the Livermore 90-in. variable-energy cyclotron. The energy resolution of the beam was about 0.5%.

F^{19} targets were thin Teflon (CF_2) films of 0.59

† Work performed under the auspices of the U. S. Atomic Energy Commission.

[1] J. L. Yntema, in *Proceedings of the Rutherford Jubilee International Conference, Manchester, 1961*, edited by J. B. Birks (Heywood and Company, Ltd., London, 1961), p. 513.
[2] A. G. Blair, in Argonne National Laboratory Report No. ANL-6878, 1964, edited by F. E. Throw, p. 115 (unpublished).
[3] R. Jahr, Phys. Rev. **129**, 320 (1963).
[4] S. Kakigi, J. Phys. Soc. Japan **20**, 1967 (1965).
[5] R. K. Sheline and K. Wildermuth, Nucl. Phys. **21**, 196 (1960).
[6] K. L. Warsh, G. M. Temmer, and H. R. Blieden, Phys. Rev. **131**, 1690 (1963).
[7] H. D. Holmgren and C. B. Fulmer, Phys. Rev. **132**, 2644 (1963).
[8] N. K. Glendenning, Ann. Rev. Nucl. Sci. **13**, 191 (1963).
[9] Sven Gosta Nilsson, Kgl. Danske Videnskab. Selskab, Mat. Fys. Medd. **29**, 1 (1955).
[10] J. P. Elliott and M. Harvey, Proc. Roy. Soc. (London) **A272**, 557 (1963).
[11] T. Inoue, T. Sebe, H. Hagiwara, and A. Arima, Nucl. Phys. **59**, 1 (1964).
[12] M. DeLlano, P. A. Mello, E. Chacon, and J. Flores, Nucl. Phys. **72**, 379 (1964).
[13] W. H. Bassichis and F. Scheck, Phys. Rev. **145**, 771 (1966).
[14] W. H. Bassichis (private communication).
[15] R. H. Siemssen, L. L. Lee, Jr., and D. Cline, Phys. Rev. **140**, B1258 (1965).

TABLE I. Integrated cross sections for the angular distributions measured for the $F^{19}(\alpha,t)Ne^{20}$ reaction at 28.5 MeV.

Ne^{20} levels	Angular interval lab system	σ (mb)
Ground state 0^+	15°–170°	0.26
1.63 MeV 2^+	15°–170°	1.65
4.25 MeV 4^+	15°–170°	0.81
4.97 MeV 2^-	15°–170°	0.07
5.63 MeV 3^-, 5.80 MeV 1^-	15°–150°	0.23
7.02 MeV 4^-, 7.19 MeV 3^-, 7.22 MeV 0^+	15°–90°	0.39

mg/cm². For absolute differential cross-section measurements, a 1.22-mg/cm² Teflon target was used. (The Teflon was mounted on two concentric aluminum rings and located at the center of a 40-in. scattering chamber. The target rotated continuously at a speed of approximately 1 cm/sec to hinder the heat deterioration of the Teflon.)

The charged particles were detected with silicon solid-state ΔE-E counter telescopes and the identifier system of Goulding *et al.*[16] Three ΔE-E telescopes were mounted in fixed positions on a curved brass arm at 10-deg intervals, which allowed measurements to be taken simultaneously at three angles. The detectors subtended a 2-deg angle, and their position could be reproduced to within 0.10 of a degree. The differential cross sections were measured from 15–170 deg in 5-deg intervals. The integrated cross sections are given in Table I.

A monitor counter placed at a fixed angle was used to obtain the correction for target-thickness variation and analyzer dead time. The identified triton signals from each of the three telescopes and the output of the monitor were stored in 200-channel subgroups of an 800-channel analyzer.

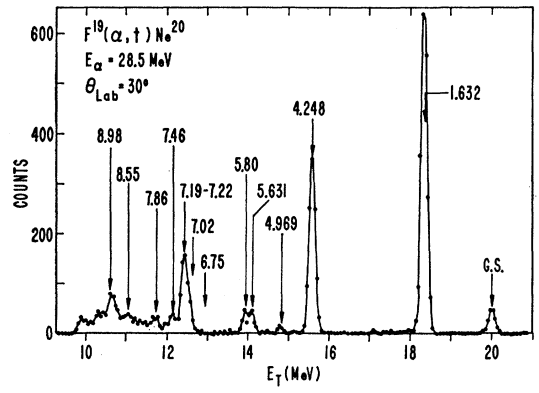

FIG. 1. Triton spectrum at 30° from the $F^{19}(\alpha,t)Ne^{20}$ reaction at 28.5 MeV.

[16] F. S. Goulding, D. A. Landis, J. Cerny, and R. H. Pehl, IEEE Trans. Nucl. Sci. **11**, 388 (1964).

EXPERIMENTAL RESULTS

A triton spectrum from the $F^{19}(\alpha,t)Ne^{20}$ reaction is shown in Fig. 1. Triton groups corresponding to the ground state, 1.63-MeV, 4.25-MeV, and 4.97-MeV levels in Ne^{20} were well separated. The triton groups leading to the 5.63-MeV and 5.80-MeV levels were not resolved. The 6.75-MeV level was barely observed at a few forward angles and did not rise above the background for all other angles. The 7.02-, 7.19-, and 7.22-MeV levels were not clearly resolved, although from the location of the 7.02-MeV peak in this group, one can infer that the 7.02-MeV level was the least excited of the three states.

The triton angular distributions shown in Fig. 2 are the results of two independent runs. The relative errors in the differential cross sections are in general not larger than 5%, while the absolute cross-section errors are of the order of 10% and are due mainly to target-thickness uncertainties.

The absolute errors for the ground-state differential cross section beyond 90° are as large as 50% because of poor statistics. In spite of the very good separation of the charged particles by the identifier system, as can be seen in Fig. 3, small numbers of deuterons can leak into the triton channel. This effect can be a source of uncertainty when the triton cross sections are small, as in the backward angles for the ground state.

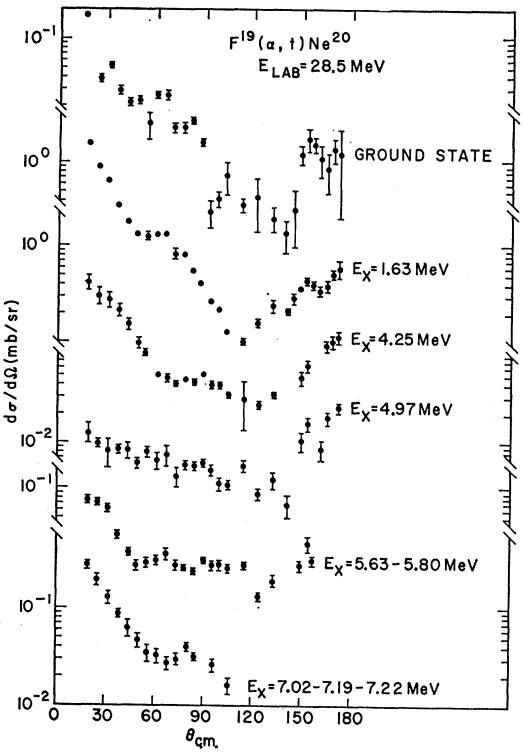

FIG. 2. Triton angular distributions from the $F^{19}(\alpha,t)Ne^{20}$ reaction to the final states indicated.

DISCUSSION OF THE DATA

The triton angular distributions to the ground state and 1.63-MeV level in Ne^{20} have a very well defined stripping character, as can be seen in Fig. 2, and the shapes of the angular distributions are very similar to those measured by Jahr[3] at 18.5 MeV.

The angular distribution of the tritons to the 4.25-MeV level is similar to the angular distribution to the first excited state, although its forward peaking is not so pronounced.

The differential cross section to the 4.97-MeV level has almost no structure. The most prominent feature here is the increase of the cross section at the backward angles.

The angular distributions to the unresolved 5.63- to 5.80-MeV levels and 7.02-, 7.19-, and 7.22-MeV levels also show forward peaking.

To compare the present data with that obtained by Kakigi[4] at 28.5 MeV, the differential cross sections to the ground, first and second excited states in Ne^{20} were integrated between 16 and 59 deg. It was found that Kakigi's values are larger by a factor of about 5.5 for all three states. Kakigi's values are also larger than those of Jahr's at 18.5 MeV, a trend that is not expected in direct reactions.

ANALYSIS OF THE DATA

The triton angular distributions were compared with zero-range DWBA calculations performed with Glendenning's "Reaction 4" code for single nucleon stripping.[8] The computation was carried out on an IBM 7094 at this laboratory.

The different (α,t) cross sections are given by

$$(d\sigma/d\Omega) \propto \frac{2J_f+1}{2J_i+1} \sum_{lm} S(l) |B_l{}^m|^2, \qquad (1)$$

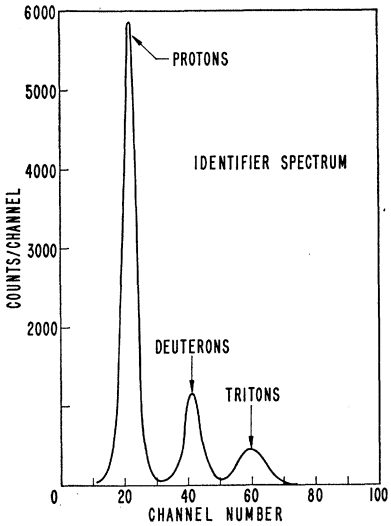

FIG. 3. Separation of the single charged particles with the identifier system.

TABLE II. Optical parameters with shallow potentials for 27.4-MeV α particles and 28.5-MeV He^3 elastically scattered from Ne^{20}.

	V (MeV)	W (MeV)	r (F)	a (F)	r_c (F)	Reference
α particles	47.0	7.4	1.806	0.592	1.25	Present work
	48.0	7.6	1.8	0.58	1.25	Fayard *et al.* (Ref. 20)
	57.5	13.2	1.75	0.560	1.4	Satchler (Ref. 19)
He^3	50.0	55.0	1.6	0.60		Aguilar *et al.* (Ref. 18)
	13.0	19.0	1.2	0.65		Gol'dberg *et al.* (Ref. 25)

where J_i and J_f are the initial spins. The $S(l)$'s are the spectroscopic factors; they depend only on the wave functions of the initial and final nuclear states. Their values will depend on which model of the nucleus is taken for their calculation. $B_l{}^m$ is the amplitude for the absorption of the proton with quantum numbers (lm):

$$B_l{}^m \propto \int [\Psi_t{}^{(-)} \phi_t \phi_l{}^m]^* V_{tp} \Psi_\alpha{}^{(+)} \phi_\alpha d\tau, \qquad (2)$$

where $\Psi_t{}^{(-)}$ and $\Psi_\alpha{}^{(+)}$ are the wave functions describing the elastic scattering, and $\phi_l{}^m$ is the bound-state proton wave function (an harmonic-oscillator wave function is used). The term ϕ_α is the internal wave function of the α particle, which is taken to be Gaussian. V_{tp} is the triton-proton interaction.

Since Glendenning's calculations do not include the evaluation of the matrix element for the formation of an α particle from a triton and a proton, the normalization factor of the theoretical cross sections given in Eq. (1) is not known. Thus, only the ratios of the spectroscopic factors could be extracted from the theoretical fits to the data.

No elastic-scattering data are available for α particles on F^{19} and tritons on Ne^{20} at the energies of this experiment. The optical parameters needed to generate the elastic-scattering wave functions $\Psi_\alpha{}^{(+)}$ and $\Psi_t{}^{(-)}$ were obtained from Kokame *et al.*[17] elastic-scattering data of 27.4-MeV α particles by Ne^{20} and Aguilar *et al.*[18] He^3 elastic-scattering data at 28.5 MeV by Ne^{20}, respectively.

Satchler[19] and Fayard *et al.*[20] have fitted Kokame's data with an optical-model calculation, and the optical parameters found by them are given in Table II. In the present work Kokame's data were also fitted, using the optical-model, least-squares search code LOKI.[21] A volume Woods-Saxon potential of the form

$$U(r) = V_c - (V+iW)(e^x+1)^{-1}, \quad x=(r-r_0A^{1/3})/a \qquad (3)$$

[17] J. Kokame, K. Fukunaga, N. Inoue, and H. Nakamura, Phys. Letters **8**, 342 (1964).
[18] J. Aguilar, W. E. Burcham, F. R. S., J. B. A. England, A. Garcia, P. E. Hodgson, P. V. March, J. S. C. McKee, E. M. Mosinger, and W. T. Toner, Proc. Roy. Soc. (London) **A25**, 13 (1960).
[19] G. R. Satchler, Nucl. Phys. **70**, 177 (1965).
[20] C. Fayard, G. Lamot, E. El-Baz, and J. Lafoucrine, Compt. Rend. **261**, 1663 (1966).
[21] E. H. Schwarcz, Phys. Rev. **149**, 752 (1966).

TABLE III. Optical parameters obtained with LOKI form a search for deep potentials for 27.4-MeV α particles (incoming channel) and 28.5-MeV He^3 (outgoing channel) elastically scattered from Ne^{20}.

	V (MeV)	W (MeV)	r (F)	a (F)	r_c (F)
Incoming channel	191.2	32.97	1.525	0.541	1.25
Outgoing channel	147.4	22.02	1.225	0.745	1.25

was used, where V_c is the Coulomb potential from a uniformly charged sphere of radius $r_cA^{1/3}$, with $r_c=1.25$ F. The optical parameters found are given in Table II, and they are very close to those found by Fayard *et al.*[20] However, of the three different sets in Table II, Satchler's parameters gave the best fit to the elastic data.

Following Rook's[22] suggestion, a search for "deep potentials" was also done with LOKI and the optical parameters obtained are given in Table III. Figure 4 shows the fit obtained with this potential compared with Satchler's fit with the shallow potential.

The only available triton elastic-scattering data was the Aldermaston data below 10 MeV.[23] The parameters obtained by Pullen *et al.*[23] for 7.2-MeV tritons on F^{19} were tried in the DWBA calculations, but the agreement with the measured (α,t) angular distributions was not good. This was expected because of the large energy difference; the tritons in this experiment are about 20 MeV.

Since it has been shown that the nuclear interactions of a proton or a neutron with a self-conjugate nucleus ($N=Z$) are identical and that the optical parameters obtained from proton elastic scattering corrected for Coulomb effects can fit equally well the neutron-scattering data,[24] it was thought reasonable to use the optical parameters obtained from fitting the He^3 elastic scattering by Ne^{20} for the outgoing channel.

The optical parameters obtained by Aguilar *et al.*[18] for the He^3 elastic scattering by Ne^{20} at 28.5 MeV were used in the DWBA calculations. Also the parameters found by Gol'dberg *et al.*[25] for the elastic scattering of He^3 between 26 and 36 MeV for nuclei ranging from Be^9 to Bi were tried. Both sets of optical parameters are given in Table II.

A search for deep potentials was also done with LOKI for Aguilar's He^3 elastic-scattering data, and the parameters obtained are given in Table III. The fit obtained with these parameters is shown in Fig. 5, together with Aguilar's fit.

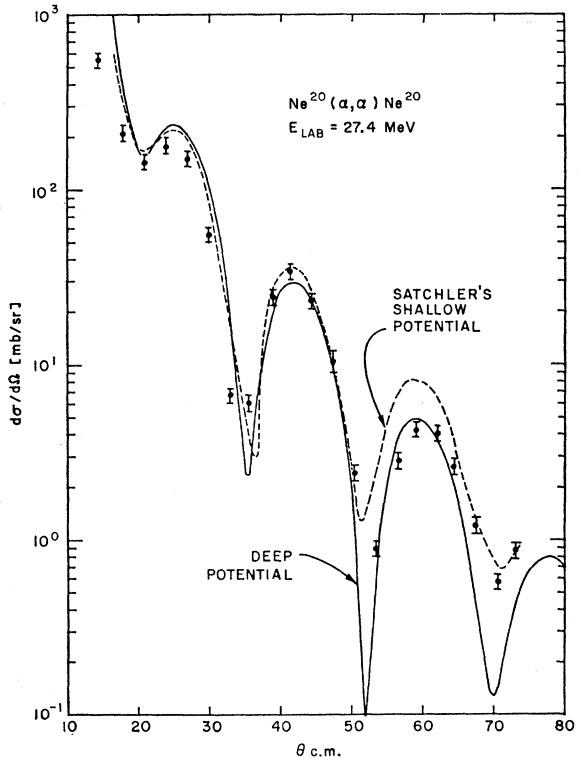

FIG. 4. Optical-model fittings with "shallow" potential (Ref. 19) and "deep" potential for the elastic scattering of 27.4-MeV α particles from Ne^{20}. The optical parameters are given in Tables II and III for the shallow and deep potentials, respectively. The experimental data are from Kokame *et al.*, Ref. 17.

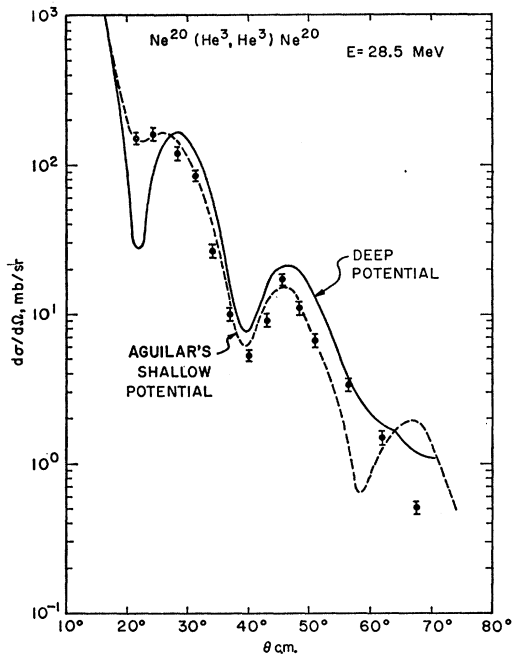

FIG. 5. Optical-model fitting with "shallow" potential (Ref. 18) and "deep" potential for the elastic scattering of 28.5-MeV He^3 from Ne^{20}. The optical parameters are given in Tables II and III for the shallow and deep potentials, respectively. The experimental data are from Aguilar *et al.* Ref. 18.

[22] J. R. Rook, Nucl. Phys. **61**, 219 (1965).
[23] D. J. Pullen, J. R. Rook, and R. Middleton, Nucl. Phys. **51**, 88 (1964).
[24] J. D. Anderson and H. F. Lutz, University of California Radiation Laboratory Report UCRL-14568, 1966 (unpublished).
[25] V. Z. Gol'dberg, V. P. Rudakov, and I. N. Serikov, Zh. Eksperim. i Teor. Fiz. **47**, 571 (1965) [English transl.: Soviet Phys.—JETP, **20**, 381 (1965)].

It is interesting that in the set of deep potentials given in Table III for the incoming and outgoing channel, the depths of the real potential for the α particles and He^3 are roughly four and three times, respectively, the single-nucleon potential (~50 MeV), in accord with Rook's[22] model of the optical potential for composite particles.

The predictions of the DWBA calculations for the (α,t) angular distributions to the ground state, 1.63- and 4.25-MeV excited states in Ne^{20} were compared with the measured cross sections by using the different optical potentials given in Tables II and III, including the combination of deep and shallow potentials. Comparisons were made also for the 4.97-MeV level with no success, which seems reasonable since the distribution showed no obvious stripping pattern.

The orbital angular-momentum transfer for these three states in Ne^{20} are 0, 2 and 4, respectively, in accordance with the selection rules.

The best fits with the shallow potentials were obtained with Satchler's[19] parameters for the α particles and Aguilar's[18] parameters for the tritons, with a radius cutoff of 3.9 F. With no radius cutoff, the agreement was slightly worse. Figure 6 shows the calculated differential cross sections with and without radius cutoff.

Better over-all agreement was found by using the deep potentials given in Table III for the same radius cutoff of 3.9 F. In Fig. 7 the DWBA calculations with these deep potentials, with and without radius cutoff, are shown. The value of 3.9 F for the radius cutoff is the same one required to fit the (He^3,d) cross sections in F^{19} in the work of Siemssen *et al.*[15]

The 4.25-MeV (4^+) Level in Ne^{20}

The triton angular distribution to the 4.25-MeV state in Ne^{20} has the features of a direct reaction (Fig. 2). If the (α,t) reaction to this level is the result of a direct single-particle stripping mechanism, then the selection rules require that the angular momentum carried by the captured proton is $l=4$. This implies that the wave function of Ne^{20} must have an appreciable amount of $1g$ component.

The calculations[9–13] presently available for the Ne^{20} wave function do not include the $(1g,2d,3s)$ shell. Thus, the value of the spectroscopic factor for the (α,t) reaction going to the 4^+ level is zero. The lack of a $1g$ component is the result of the mathematical and computing complexities in the theoretical calculation that would be incurred if it were included. It is generally believed, however, that more realistic calculations[14] will show the contribution of this component to be quite small (1–2%), thus accounting for only a small part of the experimentally measured cross section to the 4^+ level. Hence, there are grounds to speculate that there is another direct process besides the single-particle stripping, which contributes to this reaction.

A knockout mechanism has been invoked in the past[6,7] when tritons have been observed in a nuclear reaction on F^{19}. To check accurately the contribution

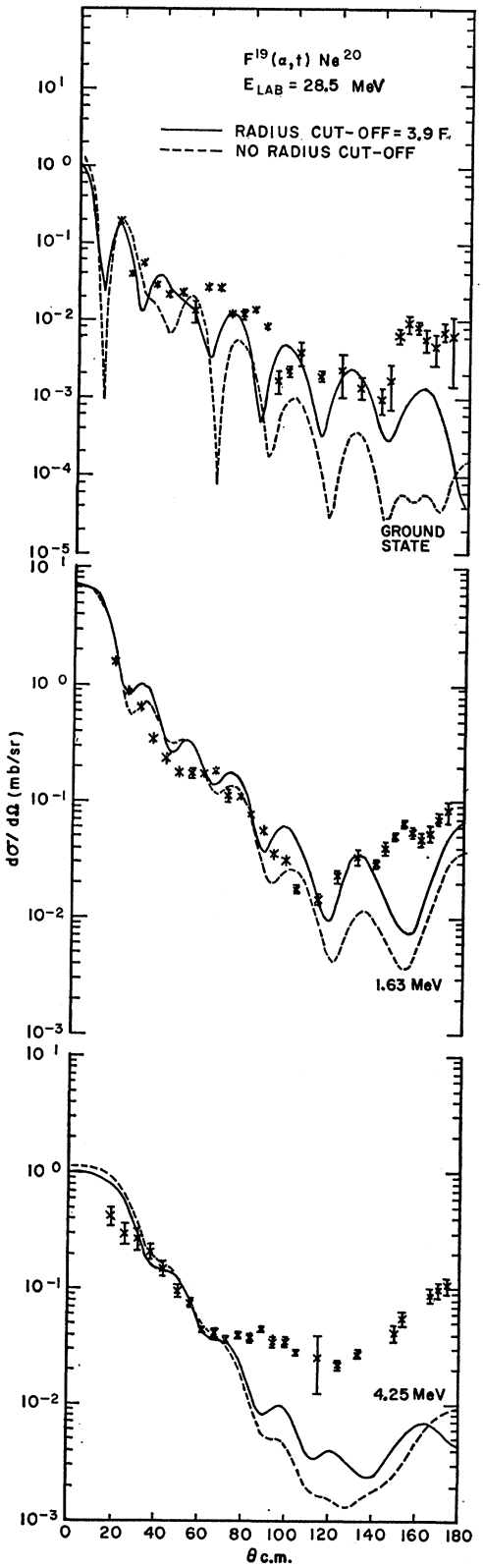

FIG. 6. DWBA stripping calculation with "shallow" potential for the triton differential cross sections from the $F^{19}(\alpha,t)Ne^{20}$ reaction at 28.5 MeV: solid curve calculated with a cutoff radius of 3.9 F; dashed curve calculated with no cutoff radius.

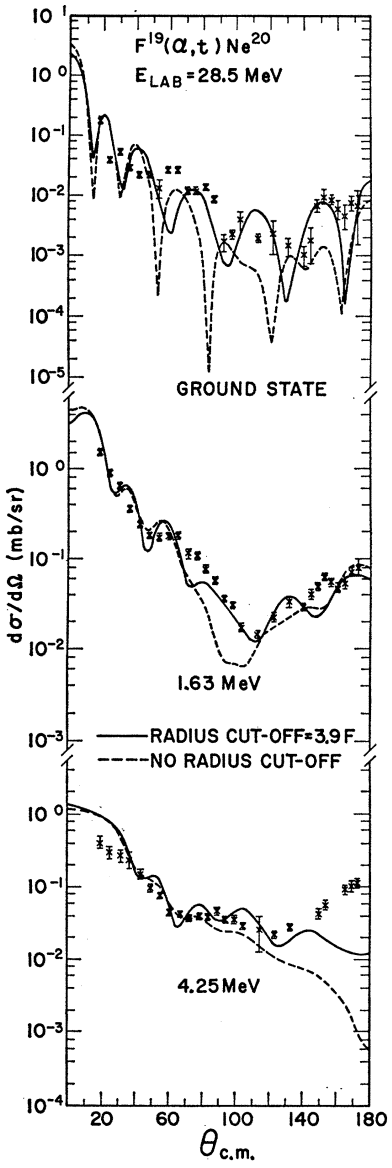

FIG. 7. DWBA stripping calculation with "deep" potentials for the triton differential cross sections from the $F^{19}(\alpha,t)Ne^{20}$ reaction at 28.5 MeV: solid curve calculated with a cutoff radius of 3.9 F; dashed curve calculated with no cutoff radius.

of knockout in the present reaction, one would have to do a finite-range DWBA calculation in which exchange integrals are included, like those being carried out by Amos *et al.*[26]

The other possible mechanism responsible for the large cross section observed for the (α,t) reaction to the 4.25-MeV state is the presence of inelastic effects in the stripping process. It has been pointed out by Penny and Satchler[27] that when nuclei show collective behavior, strong inelastic-scattering effects can be present for the incoming and outgoing particles. There is evidence[28,29] that the description of the levels below 10-MeV excitation energy in terms of rotational bands is valid for both F^{19} and Ne^{20}. The α particle can excite the $\frac{5}{2}^+$ and $\frac{3}{2}^+$ levels in F^{19} by inelastic scattering, and then the protons can be captured with $l=2$ into the 4.25-MeV (4^+) level. Alternatively, the proton can be captured with $l=2$ into the 1.63-MeV level (2^+) in Ne^{20}, followed by inelastic triton scattering to the 4.25-MeV level (stripping via core excitation[30]). In both cases proton capture with $l=2$ is allowed, and this mechanism provides a possible explanation of the large cross section observed without requiring a $1g$ component.

Kozlowsky and de-Shalit[30] have shown that the angular distributions for the stripping via core excitation are very similar in shape to those obtained for the direct single-particle stripping process. This could explain why the theoretical calculations made by using the simple stripping mechanism for this state with $l=4$ fits the shape of the experimental angular distributions reasonably well (Fig. 7).

The calculation of the stripping via core excitation to the 4.25-MeV level is being carried out by Drisko[31] and will be published elsewhere.

The 6.75-MeV (0^+) Level

The differential cross sections for the tritons to the 6.75-MeV level in Ne^{20} were estimated to be lower by a factor of 10 from the observed cross sections to the ground state. This low cross section, plus the magnitude of the background, made it impossible to obtain accurate cross-section measurements for this level.

This level has been previously observed in the $F^{19}(He^3,d)Ne^{20}$ reaction[15] at about 10 MeV and the $F^{19}(d,n)Ne^{20}$ reaction[32,33] between 2.5 and 3.56 MeV. In these two reactions, the angular distributions for the deuterons and for the neutrons showed a clear stripping pattern.

The value of $\sum_m|B_l^m|^2$ (Eq. 1) obtained from the DWBA calculation with the optical parameters given in Tables II and III for the 6.75-MeV level was about a factor of 5 lower than that obtained for the ground state. Furthermore, the same calculations for the (He^3,d) reaction at 10 MeV, using the optical parameters of Siemssen *et al.*[15] gave a value of $\sum_m|B_l^m|^2$ for the 6.75-MeV level, which was about two times larger than that for the ground state. Since the spectroscopic factors are independent of the reaction, these theoretical predictions for the (α,t) reaction at 28.5 MeV and the (He^3,d) reaction at 10 MeV show that the expected ratio of the cross sections to the 6.75-MeV level with respect to the ground state is much smaller for the first reaction. This is in agreement with the experimental results.

[26] K. A. Amos, V. A. Madsen, and I. E. McCarthy (private communication).
[27] S. K. Penny and G. R. Satchler, Nucl. Phys. **53**, 145 (1964).
[28] E. B. Paul, Phil. Mag. **2**, 311 (1957).
[29] A. E. Litherland, J. A. Kuehner, H. E. Gove, M. A. Clark, and E. Almquist, Phys. Rev. Letters **7**, 98 (1961).
[30] B. Kozlowsky and A. de-Shalit, Nucl. Phys. **77**, 215 (1966).
[31] R. M. Drisko (private communication).
[32] R. E. Benenson, H. Y. Chen, and L. J. Lidofsky, Phys. Rev. **122**, 874 (1961).
[33] R. H. Siemssen, R. Felst, M. Cosack, and J. L. Weil, Nucl. Phys. **52**, 273 (1964).

Following the semiclassical arguments of momentum mismatch,[34] a simple calculation gave for the (α,t) reaction a momentum mismatch of 5. For the (He^3,d)[15] and (d,n)[33] reactions, the values were 2 and 1, respectively. Clearly the mismatch is greatest for the (α,t) reaction.

Spectroscopic Factors

The theoretical differential cross sections shown in Figs. 6 and 7 are normalized to the measured value at one angle. As was pointed out earlier, the present calculation does not allow extracting the values of the spectroscopic factors $S(l)$ from Eq. (1). For this reason, only the value of the ratios of the spectroscopic factors for the first and second excited states with respect to the ground state were obtained. These ratios are given in Table IV for the DWBA calculations with shallow and deep potentials for a cutoff radius of 3.9 F. The values obtained with no radius cutoff are quite close in both cases.

Since the experimental evidence[29] indicates that the first three levels of Ne^{20} are the first three members of a perturbed rotational band, the spectroscopic factors for the $F^{19}(\alpha,t)Ne^{20}$ reaction to these states can be easily calculated following Satchler's[35] formalism. Satchler has derived the selection rules and the expressions for the reduced widths of stripping reactions in nuclei that exhibit collective vibrations or rotations.

The spectroscopic factor for transitions to a rotational level is given by

$$S_{jl}=g^2\frac{2I_1+1}{2I_2+1}\langle I_2K_2|I_1j\mp K_1\Omega_2\pm\Omega_1\rangle \times\langle\phi_2|\phi_1\rangle^2C^2_{Njl}(\Omega_2\pm\Omega_1). \quad (4)$$

The subscripts 1 and 2 refer to the target and final nuclear states, respectively. If either $K_1=\Omega_1=0$ or $K_2=\Omega_2=0$, g is $\sqrt{2}$; and 1 otherwise. The terms $I_{1,2}$ are the spins; $K_{1,2}$ are the projection of the spins on the intrinsic nuclear axis (Z') (Ref. 9); j is the total angular momentum of the captured nucleon; and $\Omega=|\Omega_2\pm\Omega_1|$ is the projection of j on Z'. The term $\langle\phi_2|\phi_1\rangle$ is the overlap of the initial and final vibrational states and is close to 1 for nuclei with similar deformation. The C_{jl}'s are the coefficients for the expansion of the deformed single-particle wave functions in terms of the spherical limit function. The C_{jl}'s are related to Nilsson's expansion coefficients[9] by a Clebsh-Gordan transformation.

For the specific case of the $F^{19}(\alpha,t)Ne^{20}$ reaction, the proton is captured by an even-odd nucleus and the residual nucleus is even-even. In this case,

$$K_1=\Omega_1=I_1=\tfrac{1}{2},$$
$$K_2=\Omega_2=0,$$
$$I_2=0,2,4.$$

For this set of conditions the Clebsch-Gordan coefficients in Eq. (4) and the ones relating the C_{jl}'s to Nilsson coefficients are found in Appendix IV of Satchler's paper.

If Nilsson wave functions are taken for Ne^{20}, the first three levels in the $F^{19}(\alpha,t)Ne^{20}$ reaction are formed by the capture of the proton in Nilsson orbit 6, and they are the members of the first rotational band with $K=0$. The C_{jl} coefficients can be calculated by using Nilsson's tables [9] for different values of the deformation parameter η. Because of the large $E2$ transitions within the ground-state (G.S.) rotational band of Ne^{20} $(\beta_2=0.87)$,[36] the deformation parameter is expected to be quite large $(\eta\sim8)$. Furthermore, Bishop[37] has pointed out that the measured energy levels of nuclei in the d shell are better reproduced theoretically if Nilsson wave functions are recalculated, introducing in the deformed potential a term proportional to l^2, (μl^2). The spectroscopic factors were calculated by using Bishop coefficients for $\mu=0.2$ and $\eta=6$ and 8, and their ratios are compared in Table IV with the measured ones. Also shown in the table are the ratios obtained from Harvey's[15] calculations of the spectroscopic factors for the $F^{19}(He^3,d)Ne^{20}$ reaction, using the relation between the shell model and rotational model in terms of the symmetry group $SU(3)$.[38]

TABLE IV. Ratio of the spectroscopic factors for the 1.63-MeV and 4.25-MeV levels in Ne^{20} with respect to the ground state for the $F^{19}(\alpha,t)Ne^{20}$ reaction.

Ratios	Experimental (α,t) Shallow potential	Experimental (α,t) Deep potential	(He^3,d) Ref. 15	Theoretical Nilsson model $(\mu=0.2)$ $\eta=6$	Theoretical Nilsson model $(\mu=0.2)$ $\eta=8$	$SU(3)$ Ref. 15
$(S_{1.63}/S_{G.S.})$	0.19	0.21	2.03	0.59	0.52	0.56
$(S_{4.25}/S_{G.S.})$	0.015	0.019	≤0.677	0	0	0

The large discrepancy between the values of the ratios $S_{1.63}/S_{G.S.}$ for the (α,t) and (He^3,d) reactions could be due to the poor agreement with the theoretical calculations for the ground state in both experiments. Furthermore, in the case of the (He^3,d) the authors[15] pointed out that the spectroscopic factor for the ground state was very sensitive to the choice of the optical parameters.

CONCLUSIONS

The angular distributions measured for the $F^{19}(\alpha,t)$-Ne^{20} reaction have shown that this reaction proceeds mainly through a direct-process mechanism. Although

[34] R. H. Pehl, J. Cerny, E. Rivet, and B. Harvey, Phys. Rev. 140, B605 (1965).
[35] G. R. Satchler, Ann. Phys. (N. Y.) 3, 275 (1958).
[36] P. H. Stelson and L. Grodzins (unpublished).
[37] G. R. Bishop, Nucl. Phys. 14, 376 (1960).
[38] J. P. Elliott, in *Proceedings of University of Pittsburgh Conference on Nuclear Structure, 1957*, edited by S. Meshkov (University of Pittsburgh and Office of Ordinance Research, U. S. Army, 1957), p. 298.

the stripping calculations fit the data fairly well and it is expected that stripping is the main process for the (α,t) reaction, contributions from other processes such as knockon or heavy-particle stripping (as suggested by the backward peaking in the angular distribution to the 4.97-MeV level) remain open questions. These contributions can be properly studied only when finite-range calculations are available for these processes.

The large cross section to the 4.25-MeV level is perhaps the most interesting result of this work. It should stimulate more refined theoretical calculations for the wave functions of Ne^{20} and other neighboring nuclei. The calculation of the contribution from higher configurations other than the $1d$, $2s$ shell can help to pin down the mechanism of the reaction. In particular, once these contributions of the higher shells are known, they will shed light on the role of "indirect" processes such as inelastic excitations in this reaction.

ACKNOWLEDGMENTS

The authors would like to thank Dr. R. M. Drisko for enlightening discussions, and Dr. N. K. Glendenning for the use of his DWBA code. It is a pleasure to acknowledge the assistance of the 90-in. cyclotron crew for the efficient performance of the machine, and to thank Marvin Williamson and Allan Van Lehn for the preparations of the targets.

PHYSICAL REVIEW VOLUME 158, NUMBER 4 20 JUNE 1967

Hartree-Fock Calculations with Realistic Hard-Core Potential

M. K. PAL AND A. P. STAMP

Laboratory for Nuclear Science and Physics Department, Massachusetts Institute of Technology, Cambridge, Massachusetts*

(Received 23 December 1966)

The effective matrix elements of the two-nucleon Yale potential have been used in doing Hartree-Fock (HF) calculations in $N=Z$ even nuclei ($8\leq A\leq 40$). The ground-state energy and single-particle energies and wave functions have been calculated as a function of two deformation parameters. The calculated equilibrium shapes and binding energy per nucleon are found to be reasonably good. The difficulties in the HF formalism due to the state dependence on the reaction matrix have been discussed, and methods suggested for doing a fully self-consistent calculation of the reaction matrix elements and the Hartree-Fock energy and states.

I. INTRODUCTION

ATOMIC nuclei are known to exhibit both single-particle and collective properties. An interplay of the two modes is also observed. Systems possessing similar kinds of motion have been encountered elsewhere in physics (e.g., the electron gas exhibiting collective plasma oscillation), and adequately treated in a unified theoretical frame. Similar unification has been achieved in the nuclear-structure theory in recent years.

Considerable time elapsed between the development of the unified outlook in nuclear-structure theory, and the initial proposal of the structural models: the nuclear shell model and the collective model. These models were empirical in spirit and helped to explain and systematize numerous experimental data on single-particle and collective nuclear properties, respectively. The initial understanding was handicapped by the dilemma of the successful application of the shell model on the one hand, and the strong two-nucleon interactions (having a hard-core in some states), derived from an analysis of two-body binding and scattering data, on the other. In more detailed spectroscopic calculations,[1] using the shell model, various brands of smooth well-behaved exchange-dependent potentials that are much weaker than the observed two-nucleon potentials, have been successfully used as the residual interaction between the valence nucleons. In a somewhat different approach,[2] the two-body matrix elements themselves have been treated as parameters to be determined by fitting the closed-shell plus two-nucleon nuclei, and then the spectra of neighboring nuclei calculated in terms of these matrix elements. Although such work rests heavily on the assumption of simple shell-model configurations for the nuclei under consideration, it is fairly successful in many regions of the Periodic Table. What is important here is that the effective two-body matrix elements found in such work, once again, are of fairly reasonable magnitude and bear no relation at all to the matrix elements of the "actual" two-nucleon potential (which are infinitely large because of the hard core) between shell-model states.

* Work supported in part through funds provided by the Atomic Energy Commission under Contract No. AT(30-1)-2098.

[1] J. P. Elliott and A. M. Lane, in *Handbuch der Physik*, edited by S. Flügge (Springer-Verlag, Berlin, 1957), Vol. 39, p. 241. This review article describes many spectroscopic calculations using smooth residual interactions.

[2] I. Talmi and I. Unna, Ann. Rev. Nucl. Sci. **10**, 353 (1960); I. Talmi, Rev. Mod. Phys. **34**, 704 (1962).